

# Membrane and Solution Conformations of Monogalactosyldiacylglycerol Using NMR/Molecular Modeling Methods

Kathleen P. Howard and James H. Prestegard\*

Contribution from the Department of Chemistry, Yale University, New Haven, Connecticut 06511

Received January 30, 1995<sup>⊗</sup>

**Abstract:** The conformation of uniformly <sup>13</sup>C-labeled monogalactosyldiacylglycerol (MGDG) is studied both in a membrane environment and in solution using NMR spectroscopy. Analysis of the membrane-bound conformation of MGDG is based on measurement of dipolar interactions between <sup>13</sup>C–<sup>13</sup>C and <sup>1</sup>H–<sup>13</sup>C spin pairs and on measurement of <sup>13</sup>C chemical shift anisotropies which appear in magnetically-oriented phospholipid-based membrane fragments. Potential energy maps for glycosidic torsions  $\phi$ ,  $\psi$ , and  $\theta_1$  calculated with a membrane interaction energy are used to aid in the interpretation of experimental data. The membrane-bound description for MGDG is most consistent with a set of low-energy conformations that extend the galactose headgroup away from the membrane surface. Analysis of the conformation of MGDG dissolved in CD<sub>3</sub>OD is based on measured <sup>3</sup>J<sub>CH</sub> and <sup>3</sup>J<sub>HH</sub> scalar couplings. The description of the solution conformation is modeled as a mixture of low-energy conformers predicted in the absence of a membrane interaction term and involves more extensive motional averaging than the model for MGDG embedded in the lipid matrix. Clearly the presence of a membrane interface influences preferred conformations of the galactose headgroup of MGDG when anchored to a membrane surface.

## Introduction

Over the past decade, the roles of cell-surface carbohydrates have become progressively better appreciated and understood.<sup>1</sup> The importance of glycolipids has been recognized in tumor immunology,<sup>2</sup> the inflammation response,<sup>3</sup> and membrane structure.<sup>4</sup> In many of these situations the carbohydrate portions of the glycolipids serve either as receptors for effectors of cellular function or as modulators of membrane surface properties. Therefore, the orientation of the carbohydrate residues relative to the membrane surface and the dynamic behavior of the headgroups are of fundamental interest to the biochemical community.

Monogalactosyldiacylglycerol (MGDG) is a structural component of chloroplast membranes in higher plants and of cell membranes in prokaryotic blue-green algae.<sup>5,6</sup> MGDG comprises about 50% of the total polar lipids of chloroplasts and is considered the most abundant polar lipid in nature.<sup>7</sup> Although there have been numerous physical studies of galactosyldiacylglycerols,<sup>8,9</sup> little is known concerning the molecular details of the conformation of MGDG at a membrane surface.

Studying glycolipids within a lipid lattice presents serious obstacles for the application of the most widely used methods of structural biology. Membrane systems have proven difficult to crystallize for use in X-ray diffraction studies. X-ray crystal structures of isolated glycolipids show possible minimum energy

structures, although packing constraints on headgroups are thought to induce changes in the backbone and acyl chain conformations that are not present in the physiologically-relevant liquid crystalline phase.<sup>10</sup> Solution state nuclear magnetic resonance (NMR) has been used to study membrane-bound glycolipids incorporated into small micelles or unilamellar vesicles, but broad line widths and efficient spin diffusion that accompany the relatively slow reorientation of micelle complexes complicate structural analysis.<sup>11</sup>

The most relevant structural and dynamic data on glycerolipids is derived from studies in liquid crystalline bilayers. Solid state NMR techniques have proven to be particularly useful in the study of phospholipids,<sup>12–14</sup> and glycolipids.<sup>15–17</sup> More recently, we have developed methodology utilizing magnetically-oriented phospholipid bilayers to study the conformation of membrane-bound molecules using orientational constraints derived from dipolar and quadrupolar couplings and chemical shift anisotropy data.<sup>18</sup> This methodology has been used to study the membrane-bound orientations of glycolipids prepared by synthetic methods with isotopic labels (<sup>13</sup>C, <sup>2</sup>H) at specific sites. Glycolipids studied using magnetically-oriented bilayers include a series of alkyl glycosides,<sup>19,20</sup> the sialic acid moiety

(10) Pascher, I.; Lundmark, M.; Nyholm, P.; Sundell, S. *Biochim. Biophys. Acta* **1992**, *1113*, 339–373.

(11) Siebert, H.; Reuter, G.; Schauer, R.; von der Lieth, C.; Dabrowski, J. *Biochemistry* **1992**, *31*, 6962–6971.

(12) Smith, S. O.; Kustanovich, I.; Bhamidipati, S.; Salmon, A.; Hamilton, J. A. *Biochemistry* **1992**, *31*, 11660–11664.

(13) Braach-Maksvytis, V. L. B.; Cornell, B. A. *Biophys. J.* **1988**, *53*, 839–843.

(14) Strenk, L. M.; Westerman, P. W.; Doane, J. W. *Biophys. J.* **1985**, *48*, 765–773.

(15) Skarjune, R.; Oldfield, E. *Biochemistry* **1982**, *21*, 3154–3160.

(16) Jarrell, H. C.; Jovall, P. A.; Giziewicz, J. B.; Turner, L. A.; Smith, I. C. P. *Biochemistry* **1987**, *26*, 1805–1811.

(17) Auger, M.; Van Calsteren, M.; Smith, I. C. P.; Jarrell, H. C. *Biochemistry* **1990**, *29*, 5815–5821.

(18) Sanders, C. R.; Hare, B. J.; Howard, K. P.; Prestegard, J. H. *Prog. NMR Spectrosc.* **1994**, *26*, 421–444.

(19) Sanders, C. R.; Prestegard, J. H. *J. Am. Chem. Soc.* **1992**, *114*, 7096–7107.

\* To whom correspondence should be addressed.

⊗ Abstract published in *Advance ACS Abstracts*, April 15, 1995.

(1) Drickamer, K.; Carver, J. *Curr. Opin. Struct. Biol.* **1992**, *2*, 653–654.

(2) Hakomari, S. *Curr. Opin. Immun.* **1991**, *3*, 646–653.

(3) Lasky, L. A. *Science* **1992**, *258*, 964–969.

(4) Curatolo, W. *Biochim. Biophys. Acta* **1987**, *906*, 111–136.

(5) Murphy, D. J. *FEBS Lett.* **1982**, *150*, 19–26.

(6) Quinn, P. J.; Williams, W. P. *Biochim. Biophys. Acta* **1983**, *737*, 223–266.

(7) Gounaris, K.; Barber, B. *Trends Biochem. Sci.* **1983**, Oct, 378–381.

(8) Mannock, D. A.; Brian, A. P. R.; Williams, W. P. *Biochim. Biophys. Acta* **1985**, *817*, 289–298.

(9) Sen, A.; Williams, W. P.; Quinn, P. J. *Biochim. Biophys. Acta* **1981**, *663*, 380–389.

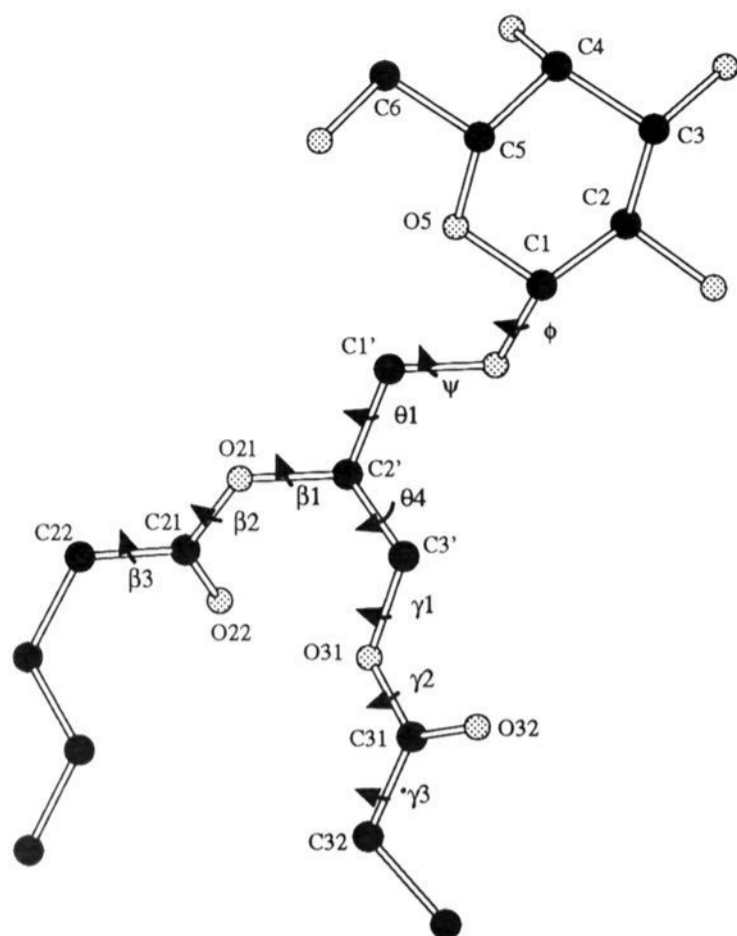


**Figure 1.** Atom numbering and notation of torsion angles. The IUPAC convention is used for numbering the sugar ring and specifying glycosidic torsions  $\phi$  and  $\psi$  (ref 56) ( $\phi = \text{O5-C1-O1-C1}'$ ,  $\psi = \text{C1-O1-C1}'\text{-C2}'$ ). To facilitate comparison of this work with that of membrane lipid structures described in recent reviews (ref 10), the atom numbering and notation of torsion angles by Sundaralingham is used for the glycerol backbone and acyl chains (ref 57). Stereospecific numbering (*sn*) labeling for the acyl chains is commonly used in related studies. In *sn* notation the  $\beta$  chain would be labeled *sn*-2, the  $\gamma$  chain *sn*-1. Throughout the text the following notation is used to denote torsion angle ranges: ap, antiperiplanar ( $180^\circ \pm 30^\circ$ ); sc, synclinal ( $60^\circ \pm 30^\circ$ ); -sc, -synclinal ( $-60^\circ \pm 30^\circ$ ).

of  $\text{G}_{\text{M}3}$ -ganglioside,<sup>21</sup> and *N*-acetylglucosamine.<sup>22</sup> Here we describe a conformational study of uniformly  $^{13}\text{C}$ -labeled MGDG prepared by biosynthetic means.

Our goal in this study is to describe the average conformation of both the glycerol backbone and galactose headgroup of MGDG in a liquid crystalline membrane environment. In liquid crystalline bilayers, membrane-bound molecules undergo rapid molecular and segmental motion and molecular interactions are perpetually broken and reformed. A complete characterization thus requires a combined motional and structural description. We have found conformations and order parameters for membrane-bound MGDG which are consistent with measured spectral parameters. See Figure 1 for the labeling of atoms and torsion angles in MGDG.

The glycerol backbone is a central part of a large family of glycerolipids which includes both phospholipids and glycolipids. The glycerol moiety occurs at the interface between aqueous and hydrophobic regions and contains three attachment sites; the polar headgroup is attached to  $\text{C1}'$  of the glycerol via an ether bond, and two hydrocarbon chains are linked via ester bonds to carbon atoms  $\text{C2}'$  and  $\text{C3}'$ . Although the conformation and dynamics of the diacylglycerol moiety of membrane lipids have received considerable attention in the literature,<sup>12,14,17,23-25</sup> the results are not entirely conclusive. Several papers call for

more work to unravel existing discrepancies. Here, dipolar couplings and chemical shift anisotropies are used to examine the properties of the glycerol backbone of MGDG in oriented bilayers.

The orientation of the saccharide headgroup is primarily determined by the conformation of the linkage between the headgroup and the glycerol moiety (torsion angles  $\phi$ ,  $\psi$ , and  $\theta_1$  in Figure 1). In this study, torsions  $\phi$ ,  $\psi$ , and  $\theta_1$  and motional averaging consistent with orientational constraints derived from the NMR data are compared with results from molecular modeling. Several studies have suggested that the membrane surface considerably reduces the range of possible conformations for the saccharide-lipid linkage.<sup>26-28</sup> The modeling protocol used here includes a membrane interaction energy.<sup>27,29</sup> In addition, the conformation of MGDG in solution is analyzed via the measurement of three-bond scalar couplings ( $^3J_{\text{CH}}$  and  $^3J_{\text{HH}}$ ) and is compared with results from the oriented membrane studies.

## Materials and Methods

**Materials.** 3-[(Cholamidopropyl)dimethylammonio]-2-hydroxy-1-propanesulfonate (CHAPSO) and L- $\alpha$ -dimyristoylphosphatidylcholine (DMPC) were purchased from Sigma Chemical Co. (St. Louis, MO). Uniformly  $^{13}\text{C}$  ( $\sim 26\%$  and  $\sim 98\%$ ) labeled algal extracts were purchased from Cambridge Isotope (Andover, MA).  $^{13}\text{C}$ -labeled MGDG was isolated from these algal extracts using flash chromatography on a series of silica gel columns eluted with 13:7:1 chloroform/methanol/ammonium hydroxide and 91:30:6:2 acetone/toluene/water/acetic acid.<sup>30</sup> All reagents used in the purification of MGDG or the preparation of NMR samples were purchased from Aldrich Chemical Co. (Milwaukee, WI).

**Preparation of NMR Samples.** Liquid crystalline NMR samples were prepared directly in 5 mm NMR tubes. A complete description of the oriented DMPC/CHAPSO system has been published elsewhere.<sup>31</sup> Briefly,  $\sim 10$  mg of  $^{13}\text{C}$ -labeled MGDG, 107 mg of DMPC, and 33 mg of CHAPSO were mixed in 350  $\mu\text{L}$  of buffer (0.1 M NaCl, 1 mM DTT, 50%  $\text{D}_2\text{O}$ , 50%  $\text{H}_2\text{O}$ ) by a combination of centrifugation, heating, cooling, and sonication until a homogeneous sample was obtained. The samples intended for magnetically-induced orientation had a lipid content of 30%. Samples were diluted to a lipid content of 20% to induce isotropic tumbling for the determination of isotropic chemical shifts and the signs of dipolar couplings.

About 5 mg of 26%- $^{13}\text{C}$ -labeled MGDG was dissolved in  $\text{CD}_3\text{OD}$  for the determination of homonuclear and heteronuclear vicinal couplings in solution.

**NMR Spectroscopy.** Proton assignments of MGDG in  $\text{CD}_3\text{OD}$  were obtained using proton homonuclear double quantum filtered coupling correlated spectroscopy (DQF-COSY).<sup>32</sup> Carbon assignments were obtained using heteronuclear multiple quantum correlation experiments (HMQC)<sup>33</sup> and heteronuclear multiple bond correlation experi-

(23) Hauser, H.; Pascher, I.; Sundell, S. In *Molecular Description of Biological Membranes by Computer Aided Conformational Analysis*; Brasseur, R., Ed.; CRC Press: Boca Raton, FL, 1990; Vol. 1; pp 267-284.

(24) Han, X.; Chen, X.; Gross, R. *J. Am. Chem. Soc.* **1991**, *113*, 7104-7109.

(25) Eklund, K. K.; Virtanen, J. A.; Kinnunen, P. K. J.; Kasurinen, J.; Somerharju, P. *J. Biochemistry* **1992**, *31*, 8560-8565.

(26) Nyholm, P.; Pascher, I. *Biochemistry* **1993**, *32*, 1225-1234.

(27) Ram, P.; Kim, E.; Thomson, D. S.; Howard, K. P.; Prestegard, J. H. *Biophys. J.* **1992**, *63*, 1530-1535.

(28) Winsborrow, B. G.; Brisson, J.; Smith, I. C. P.; Jarrell, H. C. *Biophys. J.* **1992**, *63*, 428-437.

(29) Hare, B. J.; Howard, K. P.; Prestegard, J. H. *Biophys. J.* **1993**, *64*, 392-398.

(30) Sato, N.; Murata, N. *Methods Enzymol.* **1988**, *167*, 251-259.

(31) Sanders, C. R.; Prestegard, J. H. *Biophys. J.* **1990**, *58*, 447-460.

(32) Rance, M.; Sorensen, O. W.; Bodenhausen, G.; Wagner, G.; Ernst, R. R.; Wuthrich, K. *Biochem. Biophys. Res. Commun.* **1983**, *117*, 479-485.

(33) Bax, A.; Griffey, R. H.; Hawkins, B. L. *J. Magn. Reson.* **1983**, *55*, 301-315.

(20) Sanders, C. R.; Prestegard, J. H. **1991**, *J. Am. Chem. Soc.* *113*, 1987-1996.

(21) Aubin, Y.; Ito, Y.; Paulson, J. C.; Prestegard, J. H. *Biochemistry* **1993**, *32*, 13405-13413.

(22) Hare, B. H.; Rise, F.; Aubin, Y.; Prestegard, J. H. *Biochemistry* **1994**, *33*, 10137-10148.

ments (HMBC).<sup>34</sup> Assignments of carbon resonances of MGDG in the oriented membrane samples were based on analogy to solution data and reinforced by connectivities observed in the <sup>13</sup>C–<sup>13</sup>C DQF COSY on the liquid crystalline membrane system.

The <sup>13</sup>C NMR spectra of the oriented liquid crystals were recorded on a Bruker AM-500 NMR spectrometer (125.76 MHz for <sup>13</sup>C). All spectra were acquired without sample spinning and without a field frequency lock. Waltz-16 with 40 W of power was used to achieve <sup>1</sup>H decoupling during acquisition of 1D <sup>13</sup>C–<sup>1</sup>H decoupled spectra. Acquisition times of less than 40 ms and repetition delays of at least 1.5 s were used to minimize heating of the sample. <sup>13</sup>C–<sup>13</sup>C dipolar couplings were measured using double quantum filtered experiments DQF COSY<sup>32</sup> and 2D-INADEQUATE<sup>35</sup> with low-power <sup>1</sup>H decoupling (0.5 W) for NOE during the pre-delay and high-power <sup>1</sup>H decoupling (40 W) during evolution and acquisition. Details of the experiments are provided in the figure legends.

<sup>3</sup>J<sub>HH</sub> and <sup>3</sup>J<sub>CH</sub> were measured for MGDG dissolved in CD<sub>3</sub>OD on a GE Omega NMR spectrometer (500 MHz for <sup>1</sup>H, 125.76 MHz for <sup>13</sup>C). <sup>3</sup>J<sub>HH</sub> were measured directly from a 1D <sup>1</sup>H spectrum. <sup>3</sup>J<sub>CH</sub> were measured using a 2D heteronuclear single quantum coherence experiment (HSQC)<sup>36</sup> optimized to detect long-range heteronuclear couplings. In this experiment, the delay, 2τ, used to establish the proton magnetization antiphase with respect to remote <sup>13</sup>C spins, was set to 126 ms. This was found to optimize detection of long-range couplings and null one bond heteronuclear couplings (2τ = 1/2(<sup>3</sup>J<sub>CH</sub>) = n/(<sup>1</sup>J<sub>CH</sub>)). A spin lock of 1 ms at the end of the 2τ period was used to minimize phase anomalies and unwanted <sup>1</sup>H signals.

**Analysis of NMR Data.** Both dipolar couplings and chemical shift anisotropies are a source of structural and dynamic information in anisotropic media. Dipolar couplings, *D*<sub>*ij*</sub>, may be written as follows:

$$D_{ij} = \frac{-\gamma_i \gamma_j}{2\pi^2 r^3} S_{\text{system}} S_{\text{mol}} \left( \frac{3 \cos^2 \theta - 1}{2} \right) \quad (1)$$

where  $\gamma_i$  and  $\gamma_j$  are the gyromagnetic ratios of the two interacting nuclei, *r* is the distance between coupled nuclei, and  $\theta$  is the angle between a given internuclear vector, *i*–*j*, and the bilayer normal. Net orientation and motion of the bilayer disks that comprise the liquid crystalline assemblies are included in a single order parameter, *S*<sub>system</sub>, that scales all spectral parameters. *S*<sub>system</sub> is defined as

$$S_{\text{system}} = (-1/2) S_{\text{bilayer}} \quad (2)$$

where the factor of –1/2 arises from the fact that DMPC bilayer disks orient with their normals at ~90° relative to the field and rotate rapidly about this axis. The bilayer disks also wobble about the average orthogonal direction in an axially symmetric fashion. *S*<sub>bilayer</sub> describes the residual order of the bilayer normal axes in comparison to a fully extended bilayer membrane. In our analysis *S*<sub>bilayer</sub> is assigned a value of 0.51 on the basis of the anisotropic <sup>31</sup>P shift of DMPC comprising the bulk of our lipid matrix relative to the <sup>31</sup>P shift seen in multilayer dispersions.<sup>18</sup> Over and above *S*<sub>system</sub>, experimental splittings are reduced by local molecular motions relative to the bilayer normal. *S*<sub>mol</sub> is an order parameter assigned to account for reduction of couplings due to axially symmetric motion of the membrane anchor of MGDG. Although the assumption of axially symmetric averaging is an oversimplification, the approximate cylindrical shape of MGDG suggests relatively unhindered rotation and oscillation about the most ordered director axis. Further motions about glycosidic torsion angles which can affect dipolar couplings measured from the galactose headgroup are included in the average implied by the bar over the angular term in eq 1. Averaging of the angular term is discussed in further detail in the Results.

Carbonyls at the ester linkages of MGDG have measurable chemical shift anisotropies, CSA, that can also provide useful conformational

and dynamic information. The observed chemical shift in an anisotropic system shows a dependence on order and molecular orientation which is very similar to that for dipolar coupling described above:

$$\Delta\delta = \delta_{\text{oriented}} - \delta_{\text{isotropic}} \\ = (-2/3) S_{\text{system}} S_{\text{mol}} \left[ \left( \frac{3 \cos^2 \theta_1 - 1}{2} \right) (\sigma_{11} - \sigma_{22}) + \left( \frac{3 \cos^2 \theta_3 - 1}{2} \right) (\sigma_{33} - \sigma_{22}) \right] \quad (3)$$

Here  $\sigma_{nn}$  are the principal components of the static CSA tensor and  $\theta_n$  are the angles between the *n*th CSA principal axis and the bilayer normal. In order to quantitatively employ CSA data in structural studies, both the magnitudes of the static tensor eigenvalues and the orientation of the eigenvectors within the molecular frame must be known. Although neither the magnitudes nor orientations have been measured for MGDG, values derived from suitable model compounds can be used. The principal values of the <sup>13</sup>C carbonyl tensor were taken from the experimentally determined <sup>13</sup>C carbonyl chemical shift tensor for distearylphosphatidylcholine monohydrate<sup>37</sup> and the principal axes from solid dimethyl oxalate.<sup>38</sup> The orientations of the principal axes corresponding to  $\sigma_{22}$  and  $\sigma_{11}$  are in the plane containing C21=O22 and C21–O21, with  $\sigma_{22}$  approximately along the C=O bond. The orientation of the principal axis corresponding to  $\sigma_{33}$  is nearly perpendicular to this plane.

**Molecular Modeling.** Conformational energy maps as a function of the torsion angles of the saccharide–glycerol linkage,  $\phi$ ,  $\psi$ , and  $\theta_1$ , were calculated with AMBER 4.0.<sup>39</sup> A starting conformation for MGDG was obtained by linking the crystal structure of methyl-β-D-galactose<sup>40</sup> to the diacylglycerol moiety of a low-energy structure for DMPC (molecule 2, DMPC2<sup>41</sup>). Similarity in the chemical shifts and multiplet patterns for the glycerol protons of MGDG and DMPC in solution suggests that the glycerol backbone of DMPC is likely to be similar to the backbone of MGDG and could be useful in building starting conformations for MGDG. A recent review summarizes all single crystal structures of glyceromembrane lipids and provides insight into the possible departures from this single energy minimum conformation.<sup>10</sup> All staggered rotamers of  $\theta_1$  about the C1'–C2' bond are in fact represented in glycerophospholipid crystal structures. Our analysis therefore takes into account all three possible conformers of  $\theta_1$ . Three families of starting structures (one for each of the staggered conformations of  $\theta_1$ ) were generated by rotation of the  $\phi$  and  $\psi$  torsion angles at 20° intervals using the MULTIC option of MacroModel V3.1.<sup>42</sup> The starting structures were then input into AMBER, and energy minimization was performed at each grid point to generate relaxed energy maps. Minimization included all degrees of freedom except for the torsion angles defining the respective grid point. After 5000 cycles of steepest descent, conjugate gradient minimization was used to achieve a convergence criterion of 0.05 kcal/mol. A force field with improved parameterization for oligosaccharides was utilized.<sup>43</sup> Partial charges were assigned as discussed previously.<sup>43</sup>

Two sets of energy maps were produced; one corresponds to conformers in a solution environment, the other to conformers in a membrane-bound environment. For both the solution and the membrane maps a distance-dependent dielectric constant with a proportionality factor for 4 was used to model intramolecular electrostatic interactions. An additional energy term representing the interaction of a glycolipid with a lipid bilayer–water interface is included in the calculation of the membrane maps.<sup>27,29</sup> The membrane interaction term is included in the target energy function in AMBER and calculates an

(37) Cornell, B. A. *Chem. Phys. Lett.* **1980**, *72*, 462–465.

(38) Cornell, B. A. *J. Chem. Phys.* **1986**, *85*, 4199–4201.

(39) Pearlman, D. A.; Case, D. A.; Caldwell, J. C.; Seibel, G. L.; Singh, C.; Weiner, P.; Kollman, P. A., University of California, San Francisco, 1991.

(40) Takagi, S.; Jeffrey, G. A. *Acta Crystallogr.* **1978**, *B34*, 2006–2010.

(41) Vanderkooi, G. *Biochemistry* **1991**, *30*, 10760–10768.

(42) Still, W. C., Department of Chemistry, Columbia University, New York, 1990.

(43) Scarsdale, J. N.; Ram, P.; Prestegard, J. H. *J. Comput. Chem.* **1988**, *9*, 133–147.

(34) Bax, A.; Summers, M. F. *J. Am. Chem. Soc.* **1986**, *108*, 2093–2094.

(35) Mareci, T. H.; Freeman, R. *J. Magn. Reson.* **1982**, *48*, 158–163.

(36) Bodenhausen, G.; Ruben, D. J. *Chem. Phys. Lett.* **1980**, *69*, 185–189.

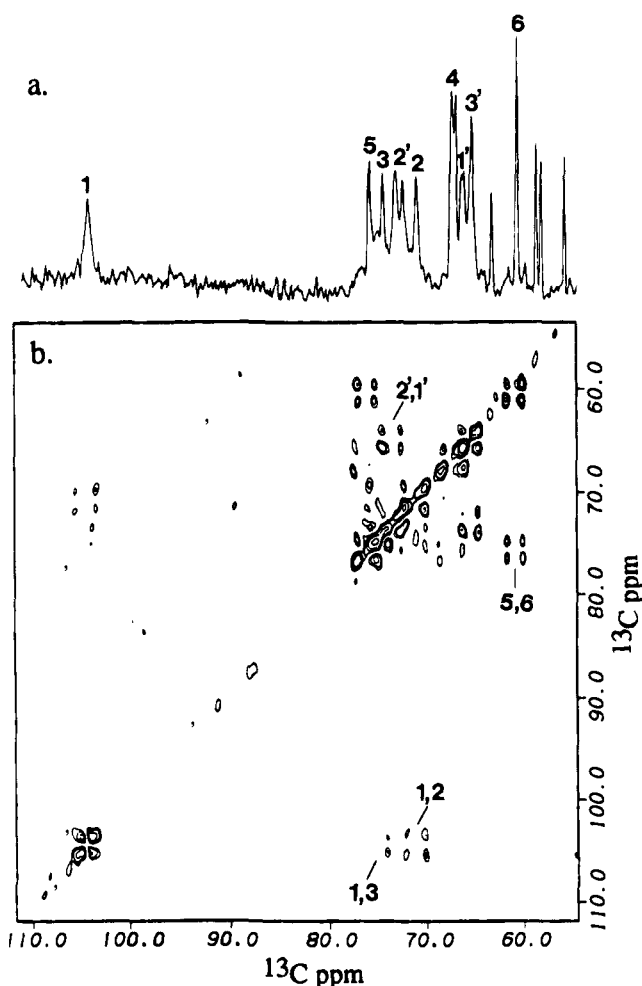


**Figure 2.** (a) Sugar/glycerol region of the  $^{13}\text{C}$ - $^1\text{H}$  decoupled spectrum of 26%- $^{13}\text{C}$ -U MGDG dissolved in 30% w/v DMPC/CHAPSO (3:1) recorded at 305 K. The spectrum was processed using 10 Hz of exponential line broadening. (b) Sugar/glycerol region of  $^1\text{H}$  decoupled DQF-COSY recorded at 305 K of the same sample described in (a). The spectrum was collected using 128 t1 points with 1152 scans per experiment. The sweep width was 26 315 Hz in t2 dimension and 8511 Hz in t1 dimension.

energy of cavity creation and an energy from dipole-induced dipole interactions in a medium of variable dielectric constant. All calculations were carried out on a Silicon Graphics Indigo workstation.

## Results

$^{13}\text{C}$ -labeled MGDG was reconstituted into a DMPC/CHAPSO model membrane system that spontaneously oriented with the bilayer normals of the membrane disks perpendicular to the applied magnet field when placed in a 11.7 T magnet (125.6 MHz for  $^{13}\text{C}$ ) at 305 K. Figure 2a shows the sugar/glycerol region of a  $^1\text{H}$  decoupled  $^{13}\text{C}$  spectrum of 26%  $^{13}\text{C}$ -labeled MGDG reconstituted in DMPC/CHAPSO. The spectrum is dominated by sites having no directly bonded  $^{13}\text{C}$ -labeled neighbors and hence presents approximately one dominant peak for each carbon in the MGDG molecule with low-amplitude  $^{13}\text{C}$ - $^{13}\text{C}$  satellites near the base of each peak. Interference due to peaks from isolated sites and from natural abundance sites in the supporting lipid matrix prevents measurement of a large number of couplings directly from this 1D spectrum.

### Measurement of Dipolar Couplings in Oriented Media.

Double quantum filtered spectroscopy was used to measure  $^{13}\text{C}$ - $^{13}\text{C}$  correlations without interference from the natural abundance  $^{13}\text{C}$  signals from the lipid matrix and single site labels

**Table 1.** Dipolar Couplings and CSAs Measured for MGDG Dissolved in DMPC/CHAPSO 3:1 at 305 K

	Dipolar Couplings		
	measured <sup>a</sup> (Hz)	corrected <sup>b</sup> (Hz)	predicted <sup>c</sup> (Hz)
Galactose Headgroup			
C1-C2	250  ± 50	205 ± 50	209
C1-C3	95  ± 50	95 ± 50	54
C3-C4	-205 ± 50	-250 ± 50	-282
C5-C6	-205 ± 25	-250 ± 25	-298
C1-H1	+1416 ± 200	1257 ± 200	1256
Backbone Region			
C1'-C2'	227  ± 50	182 ± 50	199
C2'-C3'	183  ± 50	138 ± 50	176
C21-C22	164  ± 50	-209 ± 50	-234
C31-C32	109  ± 50	-154 ± 50	-167
CSA Data			
	measured (ppm)	predicted (ppm)	
C21	-2.1 ± 1.2	-1.6	
C31	-5.1 ± 1.2	-4.8	

<sup>a</sup> Dipolar couplings measured from DQF-COSY and 2D-INADEQUATE are absolute values. Error bars are set to approximately 1/2 the line width. <sup>b</sup> Corrected values have been adjusted to eliminate the effects of scalar coupling ( $^1J_{\text{CC}} = 45$  Hz and  $^1J_{\text{CH}} = 159$  Hz). The signed set that gave the best fit solutions is listed. <sup>c</sup> The predicted values are a representative set from the best fit solution family using a square well model for motional averaging of  $\phi$  and  $\psi$  and variable populations for the three minima for  $\omega_1$ . ( $\phi = 305^\circ$ ;  $\psi = 210^\circ \pm 60^\circ$ ;  $\theta_1$ ,  $\alpha = 100\%$ ; director  $15^\circ$  tilt from *sn*-1 long axis;  $S_{\text{mol}} = 0.62$ .) The conformation corresponding to the predicted values is pictured in Figure 5.

from MGDG. Figure 2b shows a  $^1\text{H}$  decoupled DQF-COSY spectrum of 26%- $^{13}\text{C}$ -U (U = uniformly labeled) MGDG in oriented DMPC/CHAPSO bilayers. It is clear that several  $^{13}\text{C}$ - $^{13}\text{C}$  couplings can be measured from the crosspeaks. Note that some of these are quite large and both directly bonded and long-range couplings can be detected. Along the row and column corresponding to the anomeric C1 resonance, both the C1-C3 and C1-C2 couplings (95 and 250 Hz, respectively) can be seen. Other couplings were measured with the aid of 1D and 2D INADEQUATE spectra, and the use of  $^1\text{H}$  coupled spectra, as detailed in previous work.<sup>19</sup> Four  $^{13}\text{C}$ - $^{13}\text{C}$  couplings for the backbone region were measured (Table 1). Two of the couplings, C1'-C2' and C2'-C3', provide information on the orientation of the glycerol backbone. Couplings were also measured between the carbonyl carbon and the first carbon for both of the acyl chains (C21-C22, C31-C32). These provide orientational information on the initial segments of the acyl chains. Five dipolar couplings were measured for the galactose headgroup, four  $^{13}\text{C}$ - $^{13}\text{C}$  couplings and one  $^{13}\text{C}$ - $^1\text{H}$  coupling.

The observed coupling results from the addition of dipolar and scalar contributions,  $D_{ij}$  and  $J_{ij}$ , respectively. Given the  $3 \cos^2 \theta - 1$  dependence of the dipolar component, dipolar couplings can be either positive or negative, and determination of the sign greatly enhances the utility of the coupling data. Dipolar couplings scale with overall order while scalar couplings can often be assumed to be fixed and of known sign. Therefore, if one can systematically vary the order in the system by changing the temperature or concentration of components,<sup>18</sup> one can selectively scale down the dipolar coupling contribution to the observed coupling and determine the sign.

The C5-C6 splitting is well-resolved in the 1D  $^{13}\text{C}$ - $^1\text{H}$  decoupled spectrum of 98%- $^{13}\text{C}$ -U MGDG in 20% w/v DMPC/CHAPSO (3:1) at 305 K (Figure 3). Cooling the sample from 305 to 292 K causes the disks to tumble isotropically.<sup>18</sup> This averages dipolar coupling to 0 at 292 K. As we approach this

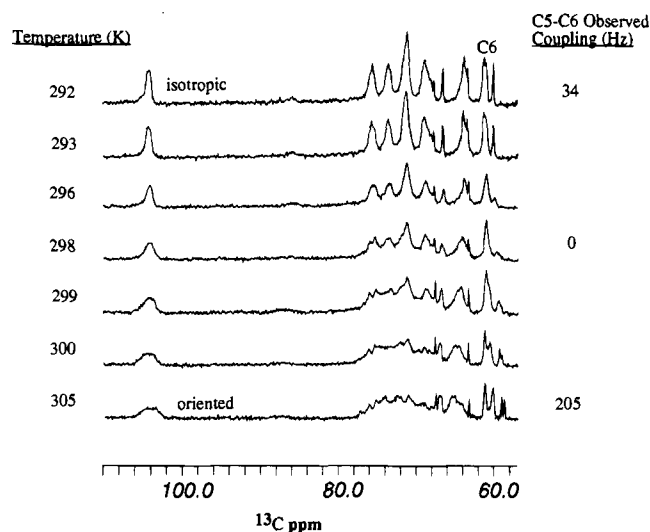


**Figure 3.** Temperature course of the  $^{13}\text{C}$ - $^1\text{H}$  decoupled spectra of 98%  $^{13}\text{C}$ -U MGDG dissolved in 20% w/v DMPC/CHAPSO (3:1). The spectra were processed using 10 Hz of exponential line broadening.

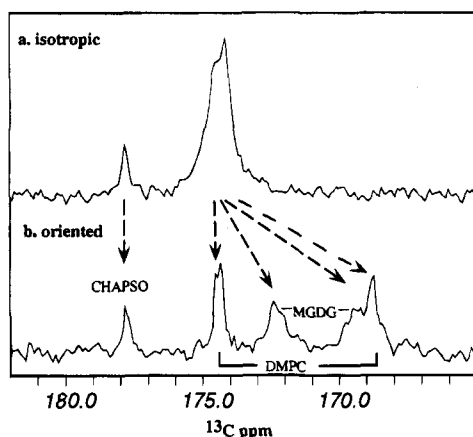


**Figure 4.** (a) Carbonyl region of the  $^{13}\text{C}$ - $^1\text{H}$  decoupled spectrum of 26%  $^{13}\text{C}$ -U MGDG dissolved in 30% w/v DMPC/CHAPSO (3:1) at 305 K. The spectrum was processed using 10 Hz of exponential line broadening. (b) Carbonyl region of the  $^{13}\text{C}$ - $^1\text{H}$  decoupled spectrum of 26%  $^{13}\text{C}$ -U MGDG dissolved in 20% w/v DMPC/CHAPSO (3:1) at 292 K. The spectrum was processed using 10 Hz of exponential line broadening.

point, the 205 Hz doublet at the C6 resonance collapses to a single peak and then splits to reach a 34 Hz scalar coupling at 292 K. This indicates a negative value for the C5-C6 coupling. The sign for the C1-H1 dipolar coupling was similarly determined from the temperature dependence of the C1-H1 splitting in a series of 1D  $^{13}\text{C}$ - $^1\text{H}$  coupled spectra of 26%  $^{13}\text{C}$ -U MGDG in 20% w/v DMPC/CHAPSO (3:1). Although the other carbon resonances for which couplings could be measured in 2D experiments were not well enough resolved in the 1D  $^{13}\text{C}$ - $^1\text{H}$  decoupled spectra to determine the signs, the C3-C4 vector is nearly collinear with C5-C6. The C3-C4 coupling was therefore assigned a negative value as well.

**Measurement of Chemical Shift Anisotropies in Oriented Media.** CSAs were measured for both of the carbonyl carbons of MGDG. Expansions of the carbonyl region of the  $^{13}\text{C}$ - $^1\text{H}$  decoupled spectra of MGDG in DMPC/CHAPSO under conditions where the system is oriented and under conditions where the bilayer fragments are tumbling isotropically are shown in Figure 4. In the isotropic spectrum, the carbonyl peaks from DMPC and MGDG are under the broad peak at 174.4 ppm and the CHAPSO carbonyl resonates at 177.0 ppm. Under conditions where the sample orients, resonances shift because of

incomplete averaging of chemical shift anisotropy. The two MGDG carbonyl resonances shift upfield to 169.4 and 172.3 ppm. The  $\beta$  chain DMPC carbonyl remains at the isotropic position whereas the  $\gamma$  chain DMPC carbonyl is shifted significantly upfield to 168.8 ppm. The positions of the DMPC carbonyls provide an internal control on overall order of the liquid crystal matrix.<sup>44</sup> (The doublet nature of the  $\beta$  chain DMPC carbonyl resonance has been established to arise from intramolecular dipolar coupling to the headgroup  $^{31}\text{P}$ .)<sup>44</sup>

**Analysis of Spectral Parameters for Membrane-Bound Molecules.** In order to interpret the above data, a search for orientations and motional models consistent with observation was executed. This was done stepwise beginning with the glycerol backbone of the glycolipid. We first tested the simplest possible assumption, namely, that a simple rigid conformation taken from a crystal structure undergoing axially symmetric motion in the bilayer provides an adequate representation. To test this possibility, orientations for internuclear coupling vectors were taken from the diacylglycerol moiety of one of the conformers found in the unit cell of an energy-minimized DMPC crystal structure (DMPC 2, structure II).<sup>41</sup> Using this conformation, possible director axis orientations and axially symmetric order parameter values were searched in an attempt to reproduce the four observed backbone couplings. (Acceptable solutions were chosen on the basis of predicted values that were within half a line width of experimental values.) No solutions were found, indicating that the assumption that all four internuclear vectors were lying on a rigid segment undergoing axially symmetric motion was not strictly correct. However, elimination of one of the more remote couplings, C31-C32, and searching using only C1'-C2', C2'-C3', and C21-C22 couplings gave a series of solutions. The best solution for the director axes was chosen on the basis of the smallest tilt from the long axis of MGDG defined by the extended acyl chains. This director axis was tilted  $15^\circ$ , and  $S_{\text{mol}}$  values ranging from 0.5 to 0.625 gave acceptable solutions. The fact that the director departs slightly from the direction of the saturated extended, *all-trans* conformation of the  $\gamma$  chain seen in the energy-minimized crystal structure<sup>41</sup> is not a major concern. (There are double bonds and disorder in the chains of MGDG in the liquid crystalline state that do not exist in the energy-minimized crystal structure. In any event, the time-averaged orientations of the acyl chains are still likely to be parallel to the bilayer normal.)

In addition to our inability to include the C31-C32 coupling, the calculated director/ $S_{\text{mol}}$  set did not produce CSAs for the carbonyl resonances that agreed with experiment. However, a few rotations of torsions at the start of the acyl chains achieved conformations that predicted CSAs consistent with experimental values. Rotation about the C2'-O21 bond ( $\beta_1$  torsion from the antiperiplanar (ap) to synclinal (sc) conformer) was found to improve the fit of the predicted C21 CSA while maintaining the close fit of the C21-C22 dipolar coupling. Rotation about C21-C22, which lies approximately parallel to C2-O21, restores parallel stacking to the chains skewed by the  $\beta_1$  rotation. A  $\beta_1$  close to sc is consistent with a second conformer for DMPC found in the unit cell of the crystal structure (see DMPC 1, structure II).<sup>41</sup> Minor rotation about O31-C31 ( $\gamma_2$  from  $178^\circ$  to  $163^\circ$ ) succeeded in creating a conformation that predicted a C31 CSA and C31-C32 coupling that were consistent with measured values. Since lipid dynamics are likely to be complex, motions other than axial diffusion may be responsible in part for averaging the  $\beta$  and  $\gamma$  chain carbonyl chemical shifts. However, given that the resulting structure was so similar to

(44) Sanders, C. R. *Biophys. J.* **1993**, *64*, 171-181.

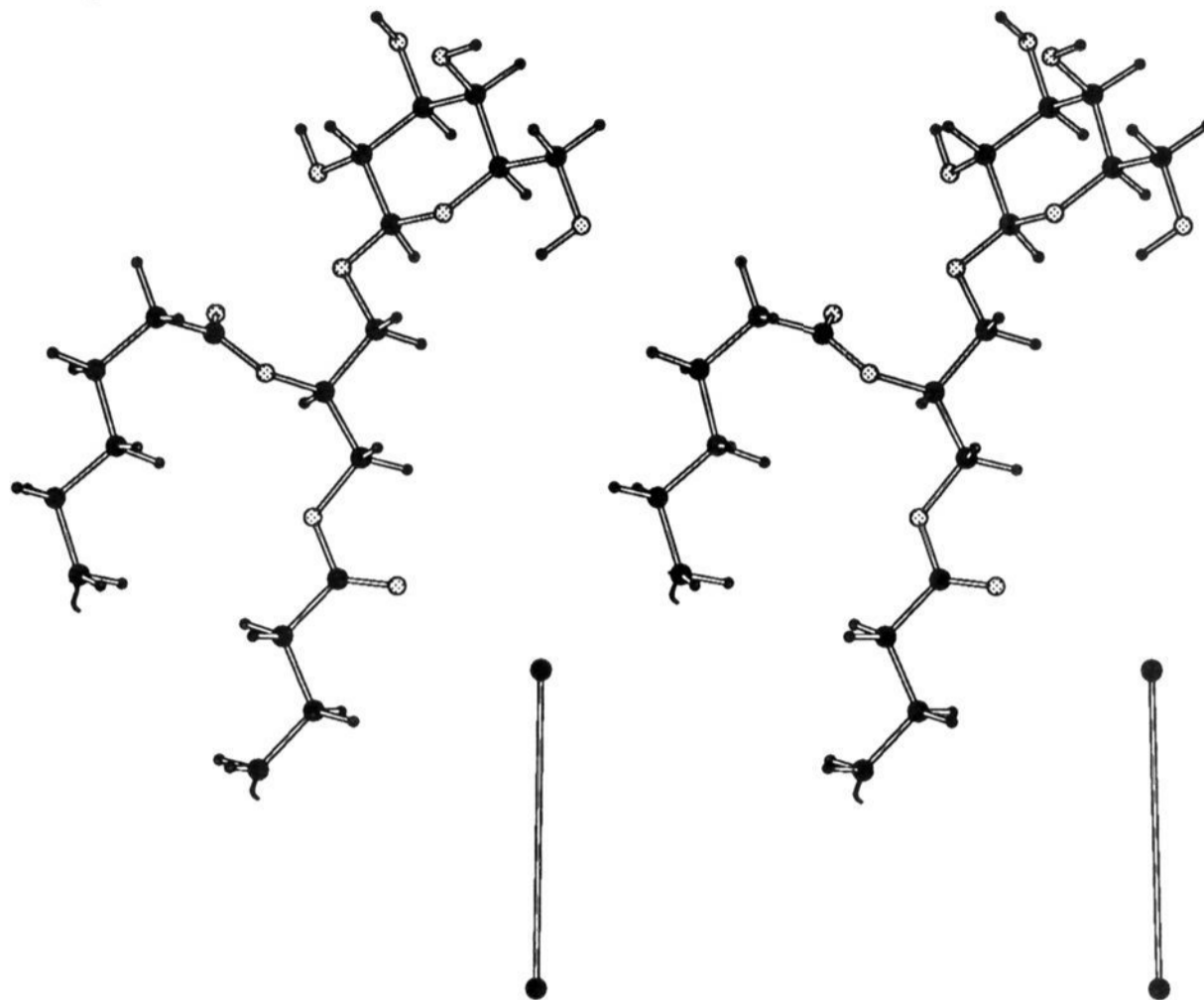


**Figure 5.** Stereo diagram of the best fit membrane-bound conformation as described in footnote *c* of Table 1.

an observed crystal structure, and given our intended emphasis on carbohydrate conformation, we felt this model for the glycerol backbone was adequate and did not feel justified in pursuing more elaborate conformational averaging models. Table 1 presents experimental and predicted values from the best fit model depicted in Figure 5.

The  $S_{\text{mol}}$  and director orientation discussed above will effect not only the glycerol backbone spectral parameters but those of the sugar as well. Analysis of dipolar couplings measured for the galactose headgroup of MGDG required consideration of averaging about the glycosidic torsions  $\phi$ ,  $\psi$ , and  $\theta_1$  as well as the effects of  $S_{\text{mol}}$  and director orientation. Dipolar couplings measured for the galactose headgroup can be expressed as averages of second-order spherical harmonics written in the laboratory frame. Wigner rotation matrices can then be used to transform the spherical harmonics from the laboratory frame through a set of frames which allows averaging about the discrete glycosidic torsions  $\phi$ ,  $\psi$ , and  $\theta_1$ .<sup>29</sup> The motions about  $\phi$  and  $\psi$  are believed to be localized within single broad minima. Thus, torsional motion around these angles was modeled using a simple square well potential. All angles within the allowed well were assumed to occur with equal probability.  $\theta_1$  is believed to sample one or more rotational states, separated by approximately  $120^\circ$ . We therefore allowed sampling of three discrete wells and treated motion about  $\theta_1$  as a weighted average over three low-energy staggered conformations (ap, sc, and -sc). Solutions were then expressed as centers and well widths for  $\phi$  and  $\psi$  and populations of the staggered conformations of  $\theta_1$ .

Conformations of the galactose headgroup of MGDG consistent with measured dipolar couplings were found using a program written in C.<sup>29</sup> Three solution families were found which centered about  $\phi/\psi$  values of  $\phi = 80^\circ/\psi = 320^\circ$ ,  $\phi = -150^\circ/\psi = 70^\circ$ , and  $\phi = -50^\circ/\psi = 210^\circ$ . Although the search for solutions allowed varying of populations of states with different  $\theta_1$  values, all three solution families had 100% population of the ap conformer for  $\theta_1$  with no mixing of either gauche conformer. Two of the three families ( $\phi = 80^\circ/\psi = 320^\circ$  and  $\phi = -150^\circ/\psi = 70^\circ$ ) produced structures with

headgroups bent back toward the backbone in ways that would suggest unfavorable steric interactions. These apparent steric violations were confirmed by molecular modeling which showed these conformations lay in regions with energy more than 5 kcal/mol above the apparent global minimum (see the Discussion and Figure 7b). However, the solution centered at  $\phi = -50^\circ/\psi = 210^\circ$  corresponds to a conformation that extends the headgroup away from the bilayer surface and has a more favorable energy. A conformation that falls within this best-fit solution family is depicted in Figure 5.

**Measurement of Spectral Parameters in Solution.** One obvious question regarding the conformation discussed above is whether this departs from the conformation normally seen in solution. Conformational studies of glycoconjugates in solution are hampered by the flexibility of glycoconjugates. Often only a small number of NOE constraints can be measured, and these can be difficult to interpret in light of conformational averaging. Long-range heteronuclear couplings across glycosidic torsions display a simpler dependence on conformational averaging than NOEs and can be a valuable tool in conformational analysis of oligosaccharides. In this study, an HSQC experiment was used to measure  $^3J_{\text{CH}}$  for both the glycosidic linkage and glycerol backbone of MGDG. The observed vicinal couplings represent simple averages of the component coupling constants for the various populated conformations.

**Vicinal Couplings for the Glycerol Backbone.** Homonuclear and heteronuclear vicinal couplings were measured for the glycerol backbone of MGDG (Table 2). Analyses of the couplings assumed motional averaging about the minimum energy staggered conformations of  $\text{C}1'-\text{C}2'$  and  $\text{C}2'-\text{C}3'$  (see Figure 6). Component coupling constants were taken from the literature<sup>45-47</sup> and are noted in the legend of Figure 6. It is clear that no one minimum for the conformation about either

(45) Hauser, H.; Pascher, I.; Sundell, S. *Biochemistry* **1988**, *27*, 9166-9174.

(46) Hansen, P. E. *Prog. NMR Spectrosc.* **1981**, *14*, 175-299.

(47) Schwarcz, J. A.; Perlin, A. S. *Can. J. Chem.* **1972**, *50*, 3667-3676.

**Table 2.** Vicinal Scalar Coupling Constants for 26%-<sup>13</sup>C-U MGDG in CD<sub>3</sub>OD at 313 K

atom pair	<sup>3</sup> J (Hz)	torsion
Glycosidic linkage		
C1'-H1	4.2	C1'-O-C1-H1
C1-H1'	3.1	C1-O-C1'-H1'
C1-H1''	3.7	C1-O-C1'-H1''
Glycerol Backbone		
C3'-H1'	3.7	C3'-C2'-C1'-H1'
H1'-H2'	4.2	H1'-C1'-C2'-H2'
C1'-H3''	2.6	C1'-C2'-C3'-H3''
H3''-H2'	2.8	H3''-C3'-C2'-H2'

C1'-C2' or C2'-C3' reproduces the coupling constants observed. A more extensive sampling of conformational space must occur.

Two couplings, <sup>3</sup>J<sub>C3'-H1'</sub> and <sup>3</sup>J<sub>H1'-H2'</sub>, provide information on the conformation about the C1'-C2' bond of the glycerol backbone, or more correctly, averaging among conformations A<sub>1'-2'</sub>, B<sub>1'-2'</sub>, and C<sub>1'-2'</sub> as depicted in Figure 6a. Populations of A<sub>1'-2'</sub>, B<sub>1'-2'</sub>, and C<sub>1'-2'</sub> of 15%, 19%, and 66% reproduce measured experimental couplings. Rotamer C<sub>1'-2'</sub>, where θ<sub>1</sub> is synclinal (sc), is the dominant conformer. In crystal structures of glyceromembrane lipids, all staggered rotamers about C1'-C2' are represented.<sup>10</sup>

Two other vicinal couplings, <sup>3</sup>J<sub>C1'-H3''</sub> and <sup>3</sup>J<sub>H3''-H2'</sub>, provide information on the conformation about C2'-C3'. Low-energy staggered conformations about C2'-C3' are pictured in Figure 6b. Populations of A<sub>2'-3'</sub>, B<sub>2'-3'</sub>, and C<sub>2'-3'</sub> of 65%, 31%, and 4% reproduce measured experimental couplings. Conformations about the C2'-C3' bond in the glycerol backbone of a series of diacylglycerol phospholipids have been studied previously using vicinal coupling constants.<sup>45</sup> Our predicted populations are closely in line with those results. Rotamer A, calculated to be the most populated conformer in solution, is also the conformer used in our previous discussion of liquid crystal data, as well as the conformation that prevails in diacylglycerol phospholipid single crystal analysis.<sup>10</sup> The dominant rotamers, A<sub>2'-3'</sub> and B<sub>2'-3'</sub>, have θ<sub>4</sub> conformers of +sc and -sc, respectively, indicating that the two oxygens on the carbon atoms C2' and C3' to which the hydrocarbon chains are attached adopt the gauche conformation where parallel alignment of the two hydrocarbon chains is readily accomplished. In contrast, in rotamer C<sub>2'-3'</sub>, these two oxygens are ap and parallel chain stacking is difficult to envisage.

**<sup>3</sup>J<sub>CH</sub> across Glycosidic Linkage.** Three vicinal coupling constants that provide information on the conformation of the glycosidic link were measured (Table 2). Fractional populations of low-energy conformations were determined which would predict coupling constants in agreement with experimentally measured values. The populated conformations were taken as the low-energy regions of molecular modeling solution energy maps, shown in Figure 7a. Five φ/ψ combinations labeled I-V (I being the lowest) correspond to low-energy regions: I (φ = -sc/ψ = sc), II (φ = -sc/ψ = ap), III (φ = sc/ψ = ap), IV (φ = sc/ψ = -sc), and V (φ = -sc/ψ = -sc). (A more complete description of the modeling is provided in the Discussion.) Values for coupling constants corresponding to these minima were taken from a study on three-bond C-O-C-H carbon-proton long-range coupling constants in carbohydrates (<sup>3</sup>J<sub>CH</sub>(ap) = 6.8, <sup>3</sup>J<sub>CH</sub>(sc) = 1.625).<sup>48</sup> A mix of the four lowest minimum conformers is needed to predict coupling constants in agreement with experiment (29% I, 22% II, 10% III, 40% IV). Hence, the solution conformation seems to sample a wider

range of conformers than is needed to fit the membrane data. The most populated conformer in solution, IV (φ = sc/ψ = -sc), is not the conformation found to dominate in the liquid crystal bilayer environment. II (φ = -sc/ψ = ap) corresponds to the conformer consistent with the liquid crystal data.

## Discussion

From the results presented above we have been able to derive structural and dynamic descriptions, both in solution and bound to a membrane phase, of one of the most abundant glycolipids in nature. While we are aware of no previous detailed description of these properties for this specific lipid, there are data on related systems, and a comparison of our description to previous work is appropriate.

**Membrane and Solution Conformations of the Glycerol Backbone Core.** We found an average membrane orientation and motion of the glycerol backbone which agrees in several respects with both experimental data and related structures in the literature. Jarrell and co-workers previously suggested, on the basis of solid state NMR data from a series of phosphoglycerolipids and glycolipids, that glycerol backbone properties were common to all glycerolipids and were determined by the lipid lattice rather than the headgroup region.<sup>16</sup> The close agreement of at least the central three-carbon fragment of our glycerol conformation with results from glycerolipids with different headgroups supports this theory. S<sub>mol</sub> values used to describe the backbone and the acyl chain core of MGDG were close to those found in the literature for the glycerol backbone of liquid crystalline diacylglycerol phospholipids and glycolipids. Several studies with several different phospholipid headgroups have determined S<sub>mol</sub> to be 0.65 ± 0.10 for the glycerol backbone.<sup>14,49</sup> The glycerol backbone of a glyceroglycolipid was also found to have a S<sub>mol</sub> of 0.65.<sup>16</sup> Jarrell and co-workers conclude that inequivalent broadening of deuterated sites on the glycerol backbone of a glyceroglycolipid indicates that motion about C1'-C2' and C2'-C3' is not free or of large amplitude since either of these situations is expected to lead to similar broadening for both C1' deuterons. Thus, they conclude that the glycerol backbone is essentially rigid on the <sup>2</sup>H NMR time scale.<sup>16</sup> This is consistent with our finding that the θ<sub>1</sub> conformation is predominantly ap, rather than a weighted average of staggered conformations.

The orientation of the glycerol backbone from the crystal structure of DMPC provides an adequate description for the analogous three-carbon glycerol fragment in MGDG. However, a rotation of ~120° about β<sub>1</sub> was required to fit the data for the initial segment of the β chain. This β<sub>1</sub> conformer is not unusual and is represented among the observed crystal structures of glycerolipids.<sup>10</sup> This conformer directs the carbonyl of the β chain toward the aqueous interface and may allow for hydrogen-bonding interactions. With this adjustment a description employing a rigid glycerol fragment and a single order parameter for the backbone seems adequate. Although this is not likely to be an accurate representation, the simplified model does provide a good fit to the experimental data and does provide a reasonable orientation and order parameter for which to build into the analysis of the glycolipid headgroup.

Vicinal couplings measured in solution for sites on the glycerol backbone allow for the determination of populations of conformers about the C1'-C2' and C2'-C3' bonds. The dominant conformation in solution for the C1'-C2' bond does not agree with that found in the best fit membrane solution. On the other hand, the dominant conformation for the C2'-C3' bond

(48) Tvaroska, I.; Hricovini, M.; Petrakova, E. *Carbohydr. Res.* **1989**, *189*, 359-362.

(49) Gally, H. U.; Pluschke, G.; Overath, P.; Seelig, J. *Biochemistry* **1981**, *20*, 1826-1831.

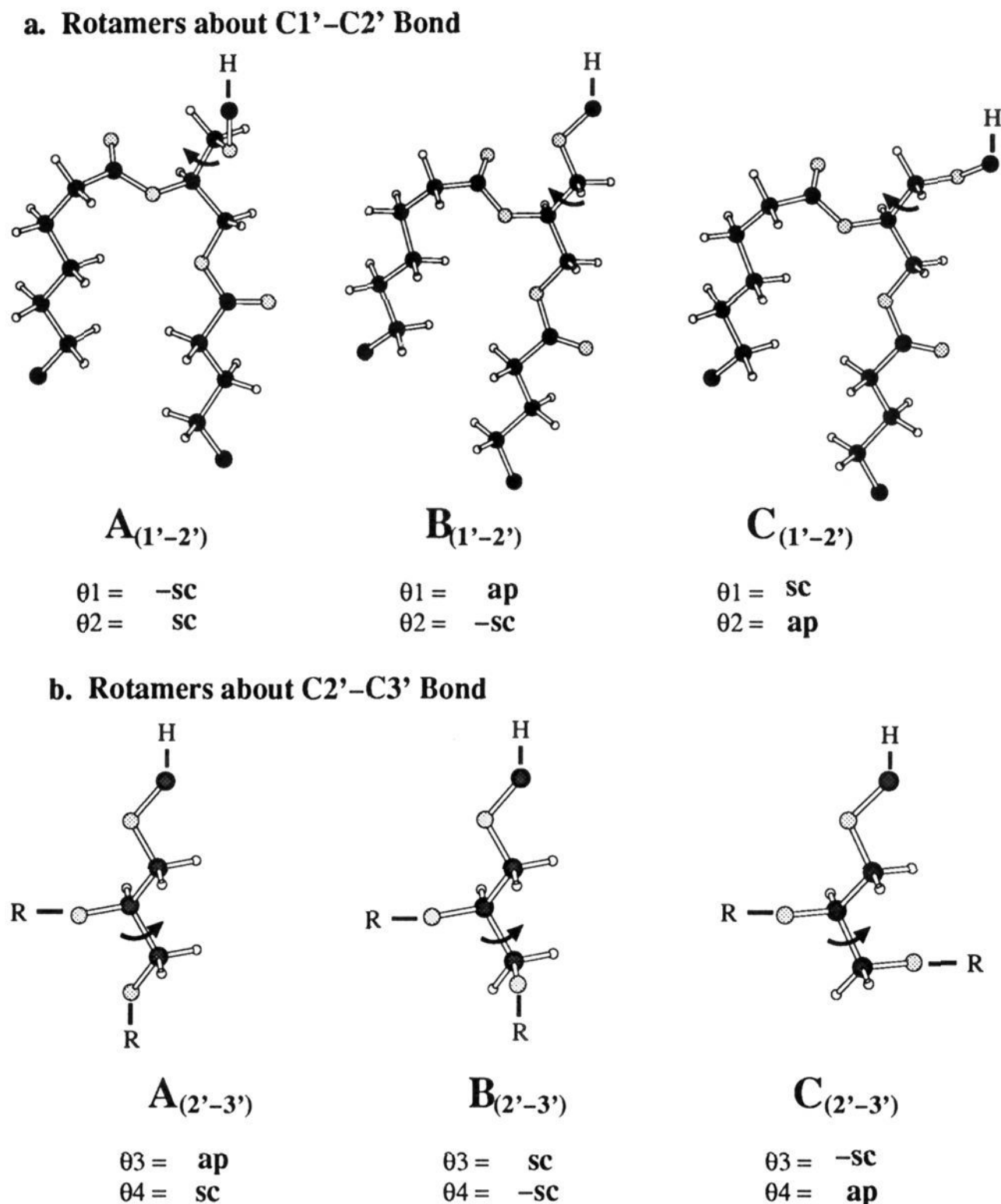


**Figure 6.** Staggered rotamers of the glycerol backbone (adapted from ref 23). H indicates the attachment of the headgroup. R indicates the attachment of acyl chains. (a) Component coupling constants used in predicting populations of rotamers for C1'-C2': A<sub>1'-2'</sub>,  $^3J_{C3'-H1'}$  = 1.65,  $^3J_{H1'-H2'}$  = 2.4; B<sub>1'-2'</sub>,  $^3J_{C3'-H1'}$  = 1.65,  $^3J_{H1'-H2'}$  = 11.7; C<sub>1'-2'</sub>,  $^3J_{C3'-H1'}$  = 4.75,  $^3J_{H1'-H2'}$  = 2.4. (b) Component coupling constants used in predicting populations of rotamers for C2'-C3': A<sub>2'-3'</sub>,  $^3J_{C1'-H3''}$  = 1.65,  $^3J_{H3''-H2'}$  = 2.4; B<sub>2'-3'</sub>,  $^3J_{C1'-H3''}$  = 4.75,  $^3J_{H3''-H2'}$  = 2.4; C<sub>2'-3'</sub>,  $^3J_{C1'-H3''}$  = 1.65,  $^3J_{H3''-H2'}$  = 11.7.

in solution does agree with that used to fit the membrane data. The population of several conformers suggests more mobility of the glycerol fragment in solution than that found in the liquid crystalline phase. Since the description of the glycerol membrane conformation in the membrane-bound state is not in terms of populations of rotamers about glycerol torsions, it is difficult to make a more direct comparison between the solution and membrane data for the backbone of this molecule.

**Membrane and Solution Conformations of the Galactose Headgroup.** The membrane-bound conformation for the galactose headgroup, as shown in Figure 5, extends the sugar headgroup away from the bilayer surface into the aqueous phase, permitting maximum hydration by bulk water molecules of the four galactose hydroxyl groups. Extension of the sugar headgroups of glycolipids essentially straight up from the bilayer surface into the aqueous region has been seen in  $^2H$  NMR studies of a glyceroglycolipid<sup>16</sup> and a glycosphingolipid.<sup>15</sup>

The glycosidic torsion angles of our best fit solution (centered at  $\phi = -50^\circ/\psi = 210^\circ$ ) are also consistent with crystal

structures of  $\beta$ -glycosides<sup>50</sup> which exhibit a preference for the  $-sc$  range for  $\phi$  (using the IUPAC definition of  $\phi = O5-C1-O1-C1'$ ). The  $\phi = -sc$  conformation is also confirmed by NMR studies of  $\beta$ -glycosides and is fully in line with the concept of the exoanomeric effect.<sup>51</sup>

Our description of the motional averaging about the average torsion angles shows minimal oscillations about the  $\phi$  torsion and considerable mobility,  $\pm 60^\circ$ , about the  $\psi$  torsion. The extremes of  $\psi$  may allow some intramolecular hydrogen bonding between the C2 hydroxyl and the  $\beta$  chain carbonyl of the backbone as has been previously suggested for certain glycolipids.<sup>26,52</sup> The model shows that the O-O distance from the C2 oxygen to the  $\beta$  chain carbonyl oxygen ranges from 2.6 to 4.6 Å as  $\psi$  ranges from  $150^\circ$  to  $270^\circ$  when  $\phi = -55^\circ$ . A distance of  $\sim 2.7$  Å would correspond to strong intramolecular hydrogen bonding.

(50) Jeffrey, G. A.; Taylor, R. *J. Comput. Chem.* **1980**, *1*, 99-109.

(51) Thøgersen, H.; Lemieux, R. U.; Bock, K.; Meyer, B. *Can. J. Chem.* **1982**, *60*, 44-57.

(52) Boggs, J. M. *Biochim. Biophys. Acta* **1987**, *906*, 353-404.



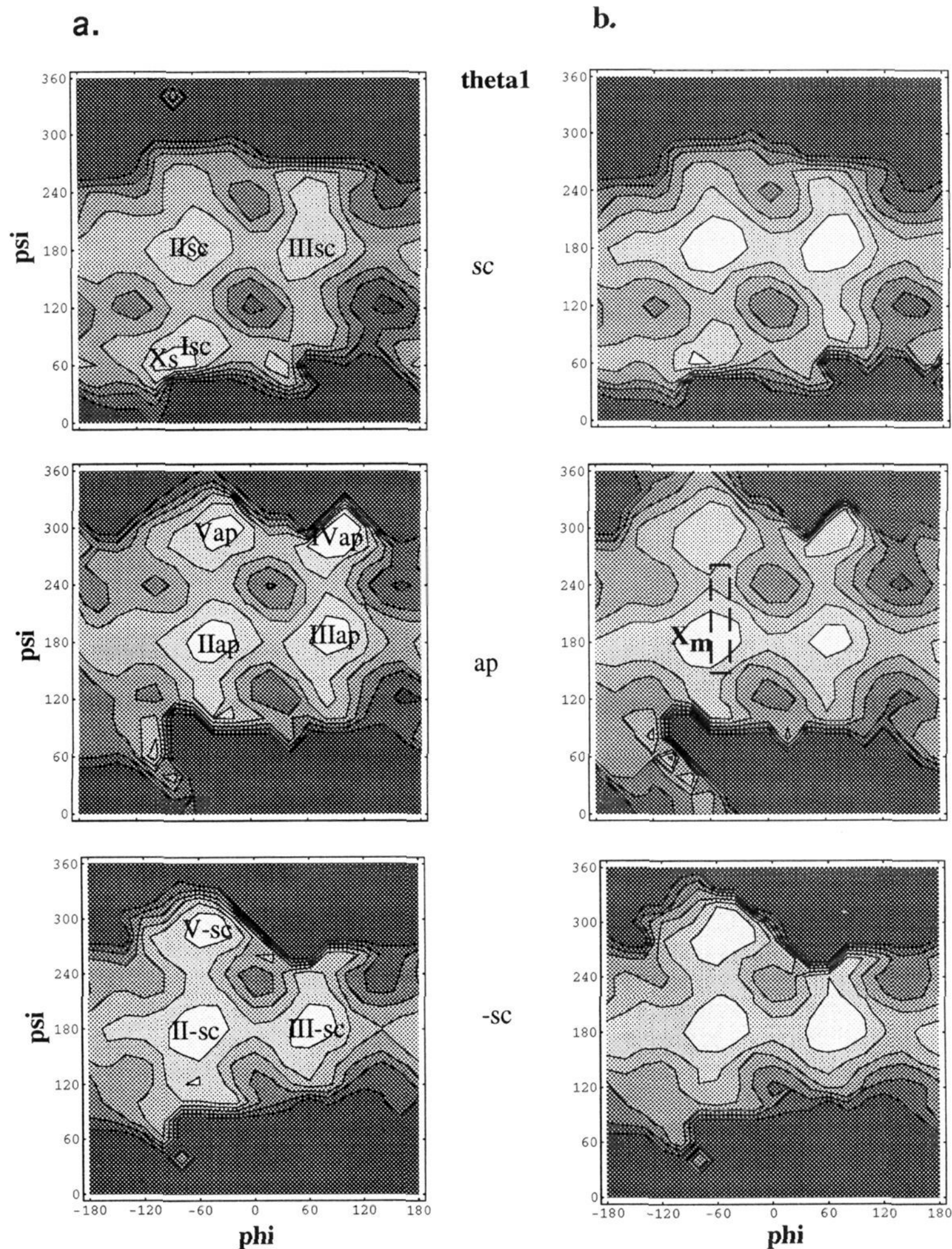


**Figure 7.** Potential energy maps for MGDG as a function of glycosidic torsions  $\phi$  and  $\psi$  for each of the three staggered conformers of  $\theta_1$ . (a) corresponds to conformers in a "solution" environment whereas (b) corresponds to conformers in a membrane-bound environment. In (a), Roman numerals correspond to the five lowest energy regions, with the global minimum marked with  $X_s$ . In (b), the dashed rectangle encompasses conformations within the range of motion for the best fit membrane-bound solution consistent with spectral parameters. The global minimum of the membrane maps is marked with a  $X_m$ . The contours are 1.8 kcal/mol apart in both (a) and (b), with the highest energy area at least 10 kcal/mol above the global minima.

The model for the glycosidic linkage consistent with the vicinal couplings measured in solution involves more extensive motional averaging than the model consistent with the headgroup conformation of MGDG embedded in the lipid matrix. This is not surprising considering torsion angles connecting individual monosaccharides in an oligosaccharide often appear to be flexible in solution, suggesting that oligosaccharides sample a variety of conformations.<sup>53</sup> Oligosaccharides may be more

ordered at the surface of a membrane because the lipid bilayer environment represents a condensed phase in which conformational interconversion could be energetically less favorable because of steric hindrance or because of specific intermolecular hydrogen bonding with neighboring molecules.

(53) van Halbeek, H.; Poppe, L. *Magn. Reson. Chem.* **1992**, *30*, S74–S86.

Other examples occur in the literature where the conformations of cell-surface carbohydrates are modulated by the presence of lipid bilayers. Jarrell and co-workers demonstrated by a solid state NMR study of a lactose-containing lipid in an aqueous, multilamellar phospholipid dispersion that the disaccharide headgroup is significantly ordered at the bilayer surface and that the conformation about the galactose–glucose intersaccharide linkage differs substantially from that found in NMR studies in solution.<sup>54</sup> Furthermore, a study of the interactions of three allelic variants of G-adhesins from *Escherichia coli* with a series of globosphingolipids demonstrated that the specificity of the adhesins for particular headgroups was greatly enhanced when the glycolipids were incorporated into natural membrane rather than conjugated to artificial surfaces.<sup>55</sup> These results suggest that the membrane may affect protein binding to glycolipids by changing the conformation of the headgroups.

**Modeling the Effect of the Membrane Surface on Glycolipid Headgroups.** A systematic way to evaluate observed conformational preferences of glycolipids is to calculate energy maps as a function of glycosidic torsions. Figure 7 shows two sets of energy maps, one without and one with a membrane interaction energy. Each set includes three maps, one for each of the staggered conformations of  $\theta_1$ . The set on the left (Figure 7a) was introduced in the Results in the analysis of vicinal scalar couplings for solution data. Five  $\phi/\psi$  combinations are labeled I–V (I being the lowest). A weighted average of four of the five minima produced a reasonable fit of our solution data.

The energy map set in Figure 7b is calculated with the same modeling protocol as the set in Figure 7a except for the addition of a membrane interaction energy. The energies contributed by the membrane interaction are on the order of a few kilocalories per mole which is comparable to variations in individual torsion potentials and most pairwise nonbonded contributions represented in AMBER. When the membrane interaction energy is added, the minima appear in the same regions of the energy maps without the membrane energy. However, the membrane interaction energy stabilizes structures at the  $\psi = 180^\circ$  strip of the  $\phi/\psi$  maps, deepening and widening the minima found in all three maps at  $\psi = 180^\circ/\phi = 60^\circ$  and  $\psi = 180^\circ/\phi = 60^\circ$ . Conformers with  $\psi$  near  $180^\circ$  tend to be extended away from the membrane surface. The net result is

that when the membrane interaction energy is added to the AMBER energy calculation, the global minimum switches from  $\psi = 50^\circ/\phi = -60^\circ$  of the  $\theta_1 = sc$  map to  $\psi = 180^\circ/\phi = -60^\circ$  of the  $\theta_1 = ap$  map. The model consistent with liquid crystalline membrane-bound data now coincides with the apparent global energy minimum. Inclusion of the membrane interaction term, therefore, clearly improves agreement between experimental and theoretical solutions.

Our molecular modeling results are consistent with a recent study which calculated conformational energy maps for a membrane-bound diacylglycerol glycolipid. A relaxed energy map of GlcDAG ( $\beta$ -D-glucosyldiacylglycerol), a closely related glycolipid to MGDG, was calculated as a function of the torsion angles of the saccharide–glycerol linkage ( $\phi$ ,  $\psi$ ,  $\theta_1$ ) using MM3.<sup>26</sup> Those maps also show a distinct preference for  $\phi = -sc$  in agreement with a strip of minima of the MGDG maps. (Nyholm and Pascher<sup>26</sup> define  $\phi$  differently as H1–C1–O1–C1, so they report the preferred  $\phi$  as  $+sc$ , which is the same as  $-sc$  for our  $\phi$  as defined in Figure 1.) Nyholm and Pascher report significant populations of  $\psi/\theta_1 = ap/ap$  (41%),  $\psi/\theta_1 = ap/-sc$  (19%),  $\psi/\theta_1 = -sc/ap$  (21%), and  $\psi/\theta_1 = +sc/+sc$  (12%) which all fall in low-energy regions of the MGDG maps calculated here. They modeled the presence of a membrane by including a restriction plane at the level of the backbone C1' to account for steric hindrance involved in translocation of the polar saccharide group into the bilayer phase. They concluded that interference of the headgroup with the membrane surface causes a considerable reduction of conformational space available for the glucose headgroup. Use of a restriction plane similar to that used in Nyholm and Pascher<sup>26</sup> would prohibit several minima in our membrane maps (i.e.,  $\phi = 60^\circ/\psi = -60^\circ$ ). Our method destabilizes these structures while still maintaining them as higher energy local minima. This intrinsic flexibility in our membrane treatment may be useful.

NMR studies of magnetically-oriented membrane fragments presented here prove to be a useful way of experimentally determining membrane-bound structures. It is clear from these studies that proximity to a membrane surface does influence glycolipid headgroup conformation. Inclusion of a membrane interface is therefore essential when designing relevant conformation studies of membrane-bound glycolipids.

**Acknowledgment.** This work was supported by the National Institutes of Health Grant GM33225. We would like to thank Drs. Brian Hare, Yves Aubin, Charles Sanders, and Julian Tirado-Rives for helpful discussions.

JA950304Z

(54) Renou, J.-P.; Giziewicz, J. B.; Smith, I. C. P.; Jarrell, H. C. *Biochemistry* **1989**, *28*, 1804–1814.

(55) Stromberg, N.; Nyholm, P.; Pascher, I.; Normark, S. *Proc. Natl. Acad. Sci. U.S.A.* **1991**, *88*, 9340–9344.

(56) I.U.P.A.C. *Pure Appl. Chem.* **1983**, *55*, 1269–1272.

(57) Sundaralingham, M. *Ann. N.Y. Acad. Sci.* **1972**, *195*, 324–355.